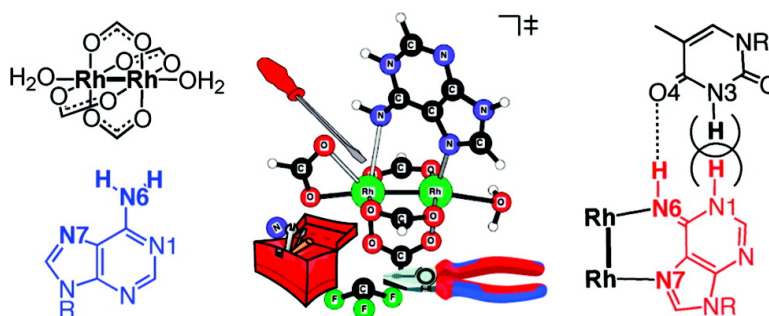


## Mechanism and Control of Rare Tautomer Trapping at a Metal–Metal Bond: Adenine Binding to Dirhodium Antitumor Agents

Dirk V. Deubel

*J. Am. Chem. Soc.*, **2008**, 130 (2), 665–675 • DOI: 10.1021/ja076603t

Downloaded from <http://pubs.acs.org> on February 8, 2009



### More About This Article

Additional resources and features associated with this article are available within the HTML version:

- Supporting Information
- Links to the 2 articles that cite this article, as of the time of this article download
- Access to high resolution figures
- Links to articles and content related to this article
- Copyright permission to reproduce figures and/or text from this article

[View the Full Text HTML](#)



# Mechanism and Control of Rare Tautomer Trapping at a Metal–Metal Bond: Adenine Binding to Dirhodium Antitumor Agents<sup>1</sup>

Dirk V. Deubel\*

Laboratory of Physical Chemistry, D-CHAB, ETH Zurich, CH-8093 Zurich, Switzerland, and  
Institute of Inorganic Chemistry, Faculty of Chemistry, University of Vienna,  
A-1090 Wien, Austria

Received September 1, 2007; E-mail: metals-in-medicine@phys.chem.ethz.ch

**Abstract:** The cause of mutations in the genome by the occurrence of nucleobases in their rare tautomeric forms was first proposed by Watson and Crick in 1953. Since this pioneering proposal, tremendous experimental and theoretical research efforts have aimed to elucidate the conditions under which nucleobase tautomerizations can occur. Previous work raised the interesting question as to whether adenine binding to the anticancer drug cisplatin can induce tautomerization of the nucleobase, but the results indicated such an event to be unlikely under physiological conditions. In this work, we have studied the reaction of three adenine (Ade) tautomers with metal–metal bonded dirhodium antitumor agents using high-level computations. The calculations reveal that the thermodynamically most stable compound in the reaction of Ade with dirhodium tetraformate in aqueous solution is a species in which a rare N6-imino tautomer spans the metal–metal bond via sites N7 and N6. However, comprehensive transition state predictions suggest that the multiple-step mechanisms leading to this bridging species are kinetically highly challenging. A number of strategies to chemically modify the metal–metal unit are considered, aiming to derive a rational plan for trapping the rare N6-imino tautomer, which is incapable of Watson–Crick pairing with canonical thymine.

## 1. Objective

Three platinum-based drugs, cisplatin, carboplatin, and oxaliplatin, are used in one of two cancer patients, but toxicity and resistance constitute significant therapeutic drawbacks.<sup>2</sup> In the current search for better metallopharmaceuticals, the metal–metal bond in dirhodium(II) complexes represents a lead structure of considerable interest.<sup>3–10</sup> Knowledge of the interactions of antitumor-active metal complexes with potential biological targets is crucial to rational drug development. It is well-known that platinum-based drugs can cross-link Gua bases or adjacent Ade/Gua bases of DNA via coordinative binding to their N7 atoms.<sup>2</sup> High-level computational studies are complementary to experimental work and revealed the transition states

for Gua and Ade binding as well as other pharmaceutically relevant reactions of cisplatin.<sup>11,12</sup>

Dirhodium(II) tetracarboxylates (DTs, Figure 1) bind to single-<sup>13,14</sup> and double-stranded<sup>15</sup> DNA as well and inhibit DNA replication<sup>16</sup> and transcription.<sup>17</sup> The presence of the metal–metal bond in dirhodium tetracarboxylate complexes opens up a great variety of nucleobase binding involving the axial (*ax*) and equatorial (*eq*) positions of the metal–metal unit (Figure 1). Gua and Ade appear to have different preferences in their binding to DTs: Early work demonstrated axial binding of Ade via site N7 (Figure 1, bottom left).<sup>18</sup> Later studies led to the

- (1) Quantum Chemical Studies of Metals in Medicine, part X.
- (2) Jung, Y.; Lippard, S. J. *Chem. Rev.* **2007**, *107*, 1387 and references cited therein.
- (3) Chifotides, H. T.; Dunbar, K. R. *Acc. Chem. Res.* **2005**, *38*, 146.
- (4) Chifotides, H. T.; Dunbar, K. R. In *Multiple Bonds Between Metal Atoms*; Cotton, F. A., Murillo, C., Walton, R. A., Eds.; Springer: New York, 2005; p 465.
- (5) Chifotides, H. T.; Dunbar, K. R. *Chem.–Eur. J.* **2006**, *12*, 6458.
- (6) Kang, M.; Chouai, A.; Chifotides, H. T.; Dunbar, K. R. *Angew. Chem., Int. Ed.* **2006**, *45*, 6148.
- (7) Angeles-Boza, A. M.; Chifotides, H. T.; Aguirre, J. D.; Chouai, A.; Fu, P. K.-L.; Dunbar, K. R.; Turro, C. *J. Med. Chem.* **2006**, *49*, 6841.
- (8) Sigel, R. K. O. *Angew. Chem., Int. Ed.* **2007**, *56*, 654.
- (9) Deubel, D. V.; Chifotides, H. T. *Chem. Commun.* **2007**, 3438. This work was featured in: Johnson, R. *Chem. Biol.* **2007**, *2*, B75.
- (10) Pruchnik, F. P. In *Metallotherapeutic Drugs and Metal-Based Diagnostic Agents*; Gielen, M., Tiekink, E. R. T., Eds.; Wiley: Chichester, U.K., 2005; p 379.

- (11) (a) Baik, M.-H.; Friesner, R. A.; Lippard, S. J. *J. Am. Chem. Soc.* **2002**, *124*, 4495. (b) Baik, M.-H.; Friesner, R. A.; Lippard, S. J. *J. Am. Chem. Soc.* **2003**, *125*, 14082. (c) Mantri, Y.; Lippard, S. J.; Baik, M.-H. *J. Am. Chem. Soc.* **2007**, *129*, 5023.
- (12) (a) Deubel, D. V. *J. Am. Chem. Soc.* **2002**, *124*, 5834. (b) Deubel, D. V. *J. Am. Chem. Soc.* **2004**, *126*, 5999. (c) Lau, J. K.-C.; Deubel, D. V. *Chem. Eur.–J.* **2005**, *11*, 2849. (d) Deubel, D. V. *J. Am. Chem. Soc.* **2006**, *128*, 1654.
- (13) (a) Asara, J. M.; Hess, J. S.; Lozada, E.; Dunbar, K. R.; Allison, J. *J. Am. Chem. Soc.* **2000**, *122*, 8. (b) Chifotides, H. T.; Koomen, J. M.; Kang, M.; Tichy, S. E.; Dunbar, K. R.; Russell, D. H. *Inorg. Chem.* **2004**, *43*, 6177.
- (14) (a) Chifotides, H. T.; Koshlap, K. M.; Pérez, L. M.; Dunbar, K. R. *J. Am. Chem. Soc.* **2003**, *125*, 10703. (b) Chifotides, H. T.; Koshlap, K. M.; Pérez, L. M.; Dunbar, K. R. *J. Am. Chem. Soc.* **2003**, *125*, 10714.
- (15) Dunham, S. U.; Chifotides, H. T.; Mikulski, S.; Burr, A. E.; Dunbar, K. R. *Biochemistry* **2005**, *44*, 996.
- (16) Erck, A.; Rainen, L.; Whitley, J.; Chang, I.-M.; Kimball, A. P.; Bear, J. L. *Proc. Soc. Exp. Biol. Med.* **1974**, *145*, 1278.
- (17) (a) Sorasaene, K.; Fu, P. K.-L.; Angeles-Boza, A. M.; Dunbar, K. R.; Turro, C. *Inorg. Chem.* **2003**, *42*, 1267. (b) Chifotides, H. T.; Fu, P. K.-L.; Dunbar, K. R.; Turro, C. *Inorg. Chem.* **2004**, *43*, 1175. (c) Aguirre, J. D.; Lutterman, D. A.; Angeles-Boza, A. M.; Dunbar, K. R.; Turro, C. *Inorg. Chem.* **2007**, *46*, 7494.

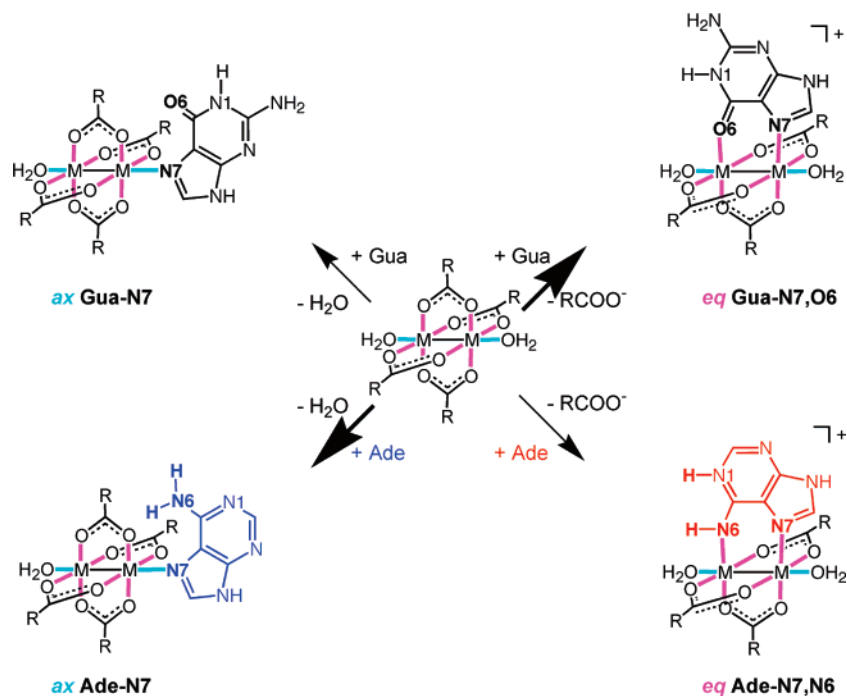


**Figure 1.** Plausible Gua (top) and Ade (bottom) adducts with dirhodium tetracarboxylates ( $M = \text{Rh}$ ). Bold arrows indicate well-characterized nucleobase binding modes.

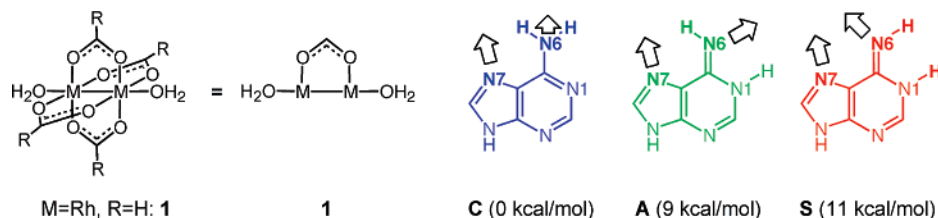


**Figure 2.** Dirhodium tetraformate (**1**) and the **C**, **A**, and **S** tautomers.<sup>25</sup> Relative free energies of the free tautomers are given in parentheses; the arrows indicate plausible metal binding sites at N7 and N6.

discovery that Gua-N7,O6 can bridge the equatorial position of the metal–metal bond (Figure 1, top right).<sup>14,19</sup> Interestingly, neither *ax* Gua-N7 nor *eq* Ade-N7,N6 species<sup>20</sup> in the aqueous chemistry of dirhodium tetracarboxylates have been reported in the literature. A recent high-level computational study<sup>9</sup> on Gua binding to DTs in aqueous solution suggested that the reaction proceeds via intermediate *ax* Gua-N7 species and finally affords the *eq* Gua-N7,O6 product.

The adenine reaction with dirhodium anticancer complexes is chemically more interesting and biologically more involved than the guanine reaction, because forming a bridging Ade-N7,N6 species would require at least one tautomerization event: Sometime during the reaction, a proton must transfer from Ade-N6 to N1, yielding an N6-imino rare tautomer.<sup>21</sup> This is displayed in Figure 1, where the canonical Ade tautomer

contains two protons at the N6 atom (blue) and the N6-imino rare tautomer contains one proton each at the N6 and N1 atoms (red). The stabilization of rare nucleobase tautomers<sup>22</sup> by metal ions and complexes has been of interest to scientists for decades.<sup>21, 23–24</sup> In previous experimental and theoretical work, it was investigated whether cisplatin binding may stabilize rare Ade tautomers, but the results show that such a stabilization occurs in vacuo<sup>24g</sup> rather than in aqueous solution.<sup>21,24c</sup>

The objective of this work is to explore the feasibility, mechanism, control, and consequence of adenine binding to dirhodium anticancer complexes. The combined density functional theory (DFT) and continuum dielectric model (CDM) approach employed herein shows the state-of-the-art balance between the level of theory and realistic models in the challenging prediction of transition states for the reactions of dinuclear anticancer complexes.<sup>9,12d</sup> We have considered the reactions of  $[\text{Rh}_2(\mu\text{-O}_2\text{CH})_4(\text{OH})_2]$  (**1**) with three relevant adenine tautomers (Figure 2): the canonical tautomer **C** and the N6-imino rare tautomers **A** and **S**.<sup>25</sup> The paper is organized as follows: *First*, we predict the stability of various adenine binding modes in the reactions of the three tautomers with **1**, and the results are compared to the analogue Gua binding.<sup>9</sup> *Second*, we investigate relevant transition states to assess which

- (18) (a) Rainen, L.; Howard, R. A.; Kimball, A. P.; Bear, J. L. *Inorg. Chem.* **1975**, *14*, 2752. (b) Farrell, N. *J. Chem. Soc., Chem. Commun.* **1980**, 1014. (c) Rubin, J. R.; Haromy, T. P.; Sundaralingam, M. *Acta Crystallogr.* **1991**, *C47*, 1712.
- (19) (a) Dunbar, K. R.; Matonic, J. H.; Saharan, V. P.; Crawford, C. A.; Christou, G. *J. Am. Chem. Soc.* **1994**, *116*, 2201. (b) Crawford, C. A.; Day, E. F.; Saharan, V. P.; Folting, K.; Huffman, J. C.; Dunbar, K. R.; Christou, G. *Chem. Commun.* **1996**, 1113.
- (20) For synthesis of  $[\text{Rh}_2(\text{DTolF})_2(9\text{-ethyladenine-N7,N6})_2(\text{NCCH}_3)](\text{BF}_4)_2$  and related compounds, see: (a) Catalan, K. V.; Mindiola, D. J.; Ward, D. L.; Dunbar, K. R. *Inorg. Chem.* **1997**, *36*, 2458. (b) Catalan, K. V.; Hess, J. S.; Maloney, M. M.; Mindiola, D. J.; Ward, D. L.; Dunbar, K. R. *Inorg. Chem.* **1999**, *38*, 3904.
- (21) Lippert, B. In *Progress in Inorganic Chemistry*; Karlin, K. D., Ed.; Wiley & Sons: New York, 2005; Vol. 54, p 385.

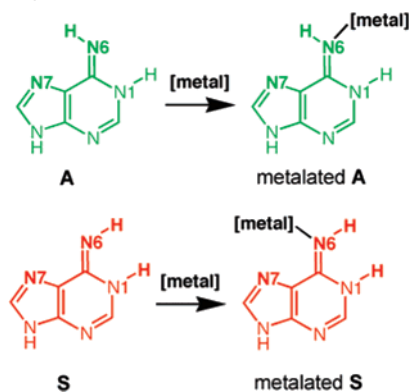
- (22) Watson, J. D.; Crick, F. H. C. *Nature* **1953**, *171*, 964.
- (23) Lippert, B. *Coord. Chem. Rev.* **2000**, *200*, 487.

nucleobase binding modes remain viable in kinetically controlled reactions. *Third*, we propose strategies as to how modifications of the metal–metal unit of the anticancer complex can control the stability of transition states and intermediates in pathways leading to metalated rare tautomers. *Fourth* and finally, we discuss biological implications of the results.

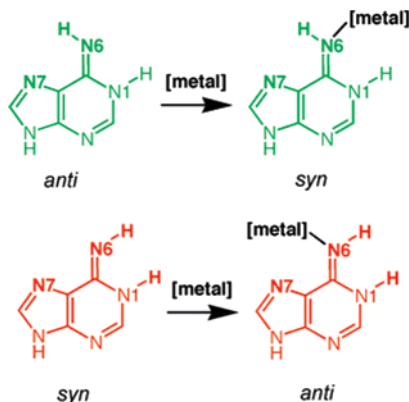
## 2. Stability of Nucleobase Binding Modes

The relative free energy (B3LYP)<sup>26,27</sup> of the free **C**, **A**, and **S** adenine tautomers in aqueous solution is predicted to be 0, 9, and 11 kcal/mol, respectively (Figure 2). This result implies that the binding of the **S** tautomer to the metal–metal unit poses a true challenge, because a rather high tautomerization free energy of 11 kcal/mol has to be compensated by the interactions

- (24) (a) Lippert, B.; Schöllhorn, H.; Thewalt, U. *J. Am. Chem. Soc.* **1986**, *108*, 6616. (b) Schöllhorn, H.; Thewalt, U.; Lippert, B. *J. Am. Chem. Soc.* **1989**, *111*, 7213. (c) Lippert, B.; Schöllhorn, H.; Thewalt, U. *Inorg. Chim. Acta* **1992**, *198–200*, 723. (d) Zamora, F.; Kunsman, M.; Sabat, M.; Lippert, B. *Inorg. Chem.* **1997**, *36*, 1583. (e) Sponer, J.; Sponer, J. E.; Gorb, L.; Leszczynski, J.; Lippert, B. *J. Phys. Chem. A* **1999**, *103*, 11406. (f) Viljanen, J.; Klika, K. D.; Sillanpää, R.; Arpalähti, J. *Inorg. Chem.* **1999**, *38*, 4924. (g) Sponer, J.; Burda, J. V.; Leszczynski, J. *J. Biol. Inorg. Chem.* **2000**, *5*, 178. (h) Velders, A. H.; van der Geest, B.; Kooijman, H.; Spek, A. L.; Haasnoot, J. G.; Reedijk, J. *Eur. J. Inorg. Chem.* **2001**, 369. (i) Hotze, A. C. G.; Broekhuizen, M. E. T.; Velders, A. H.; van der Schilden, K.; Haasnoot, J. G.; Reedijk, J. *Eur. J. Inorg. Chem.* **2002**, 369. (j) Deubel, D. V. *Angew. Chem., Int. Ed.* **2002**, *42*, 1974. (k) Anorbe, M. G.; Luth, M. S.; Roitzsch, M.; Cerda, M. M.; Lax, P.; Kampf, G.; Sigel, H.; Lippert, B. *Chem.–Eur. J.* **2004**, *10*, 1046. (l) Sigel, H. *Pure Appl. Chem.* **2004**, *76*, 1869. (m) Klika, K. D.; Arpalähti, J. *Chem. Commun.* **2004**, 666. (n) Knobloch, B.; Sigel, R. K. O.; Lippert, B.; Sigel, H. *Angew. Chem., Int. Ed.* **2004**, *44*, 3793. (o) van der Wijst, T.; Fonseca Guerra, C.; Swart, M.; Bickelhaupt, F. M.; Lippert, B. *ICBIC 13*, Vienna, Austria, 2007, P238.
- (25) In this work, we systematically denoted the N6-imino tautomers of adenine as **A** and **S** forms according to the position of the protons at N1 and N6 (Figure 2). For the sake of clarity, we find it important that the names remain unchanged when N6 is metalated.



Note that in previous work (see ref 21) the *anti* and *syn* nomenclature was frequently used for the N6-imino tautomers. Their names would change when N6 is metalated.



(26) Becke, A. D. *J. Chem. Phys.* **1993**, *98*, 5648.

(27) Lee, C. T.; Yang, W. T.; Parr, R. G. *Phys. Rev. B* **1988**, *37*, 785.

with the dirhodium complex. Still, the relative free energy of the **S** tautomer in aqueous solution is much lower than expected previously: Recent computational studies focusing on free adenine<sup>28</sup> predicted the *in vacuo* free energies of **C**, **A**, and **S** to be approximately 0, 12, and 19 kcal/mol, respectively, which is in excellent agreement with the *in vacuo* free energies we obtain. Some Ade tautomers were subjected to detailed solvation<sup>28a</sup> and electronic structure<sup>28b</sup> analyses, but the **S** tautomer was excluded from such studies, possibly because of its high free energy *in vacuo*. It turns out that this “neglected” **S** tautomer can be strongly stabilized by a metal–metal unit.

**General Considerations.** We have explored the stability of various binding modes in the reaction of the three Ade tautomers with **1**. It is important to note that some Ade tautomers do not permit all metal binding modes (see arrows in Figure 2): **S** can bind in a monodentate fashion (via N7 or N6) or in a bidentate fashion (via N7 and N6). **A** can bind only in a monodentate fashion (via N7 or N6). We thought that **C** can only bind via N7 in a monodentate fashion, but we have also investigated binding of the N6-amino group of **C**. To facilitate the presentation of the large amount of results in a compact and clear way, we have used a color coding showing the **C**, **A**, and **S** tautomers in blue, green, and red, respectively.<sup>25</sup> We present the structures of the most relevant species and their predicted free energies in aqueous solution; details of all species are given in the Supporting Information.

**Monodentate N7 Binding.** Figure 3 displays the predicted free energies for adenine N7 binding. The calculations show that the nucleobase may be either stabilized or destabilized, depending on both the tautomer (**C**, **A**, **S**) and on the coordination site at the metal (axial or equatorial). Axial (*ax*) Ade-N7 binding stabilizes the **C** and **A** tautomers but destabilizes the **S** tautomer (Figure 3, top). This is demonstrated by the free energies of **C2** (−4 kcal/mol), **A2** (7 kcal/mol), and **S2** (16 kcal/mol), as compared to the free energies of the free tautomers **C**, **A**, **S** (0, 9, 11 kcal/mol, respectively). In contrast, equatorial (*eq*) Ade-N7 binding, leading to a monodentate carboxylate, destabilizes the **C** and **A** tautomers but destabilizes the **S** tautomer only marginally (Figure 3, bottom). This is demonstrated, for example, by the free energies of **C4** (5 kcal/mol), **A4** (15 kcal/mol), and **S4** (12 kcal/mol) as compared to the free energies of the free tautomers. We find that the differential stabilization of Ade-N7 binding can be largely rationalized by intramolecular hydrogen bonding (Figure 3). For example, **C2** and **A2** benefit from a hydrogen bond involving an N6-H group and a carboxylate oxygen atom, but **S2** lacks this hydrogen bond. **S4** contains a hydrogen bond involving an axial water and the N6 atom of the nucleobase, but **C4** and **A4** lack this hydrogen bond. Our prediction that **C2** is the most stable species among all Ade-N7 adducts is consistent with experimental structures showing the same binding mode.<sup>18b,c</sup>

**Monodentate N6 Binding.** Figure 4 shows the predicted free energies for adenine N6 binding, revealing different trends as compared to N7 binding. The **A** tautomer (9 kcal/mol) experi-

(28) Relative energies of the A/S tautomers of free adenine: This work: B3LYP/6-311(d,p). *In vacuo*:  $G_{\text{vac}} = 12.4/18.7$  kcal/mol. In aqueous solution:  $G_{\text{sol}} = 9.4/10.8$  kcal/mol. (a) Hanus, M.; Kabalac, M.; Rejnek, J.; Ryjacek, F.; Hobza, P. *J. Phys. Chem. B* **2004**, *108*, 2087. MP2/TZV2P:  $G_{\text{vac}} = 12.1/18.1$  kcal/mol.  $G_{\text{sol}} = 8.5$  kcal/mol / not rep. (b) Fonseca Guerra, C.; Bickelhaupt, F. M.; Saha, S.; Wang, F. *J. Phys. Chem. A* **2006**, *110*, 4012. BP86/QZVP:  $E_{\text{vac}} = 10.6/16.5$  kcal/mol. (c) Kabelac, M.; Hobza, P. *Phys. Chem. Chem. Phys.* **2007**, *9*, 903.

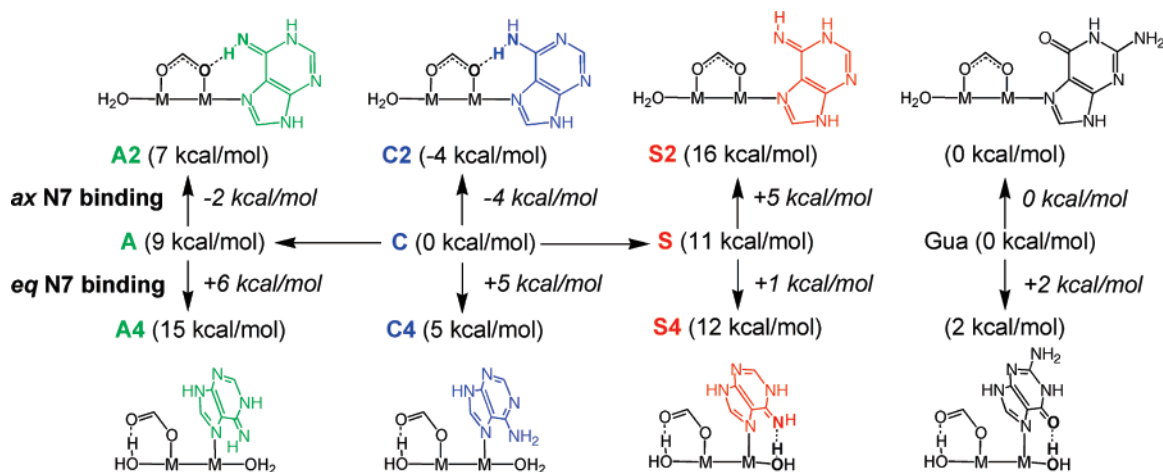


**Figure 3.** Axial and equatorial N7 binding of C (blue), A (green), S (red), and Gua (black) to **1**. Molecular free energies in parentheses; differences in italics.

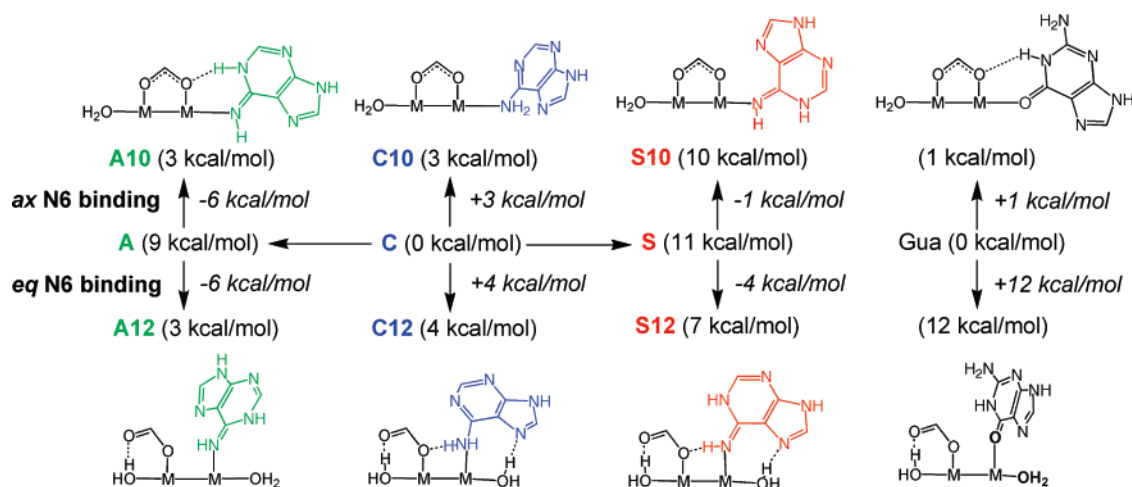


**Figure 4.** Axial and equatorial N6 binding of C (blue), A (green), and S (red) to DT. Gua-O6 binding (black) is given for comparison. Molecular free energies in parentheses; differences in italics.

ences the greatest stabilization of  $-6$  kcal/mol, when binding to the *ax* position in **A10** (3 kcal/mol) or to the *eq* position in **A12** (3 kcal/mol). The **S** tautomer (11 kcal/mol) is slightly stabilized by N6 metalation, but the metal adducts **S10** (10 kcal/mol) and **S12** (7 kcal/mol) remain relatively high in free energy. Most surprisingly, the *ax* and *eq* metal adducts of the N6-amino group of the **C** tautomer, **C10** (3 kcal/mol) and **C12** (4 kcal/mol), are thermodynamically competitive to the N6-metal adducts of the other Ade tautomers. As the N6-amino group contains two protons, and the  $\pi$  lone pair at N6 may be integrated in the delocalized  $\pi$  electrons of the nucleobase, we would have expected the N6-metalated amino species to be rather instable.

**Bidentate-Chelating and Bidentate-Bridging N7,N6 Binding.** Bidentate binding modes are only plausible for the **S** tautomer;<sup>29</sup> the predicted structures and free energies are displayed in Figure 5. The chelate **S13** (1 kcal/mol) with *eq* N6 and *ax* N7 atoms is more stable than the chelate **S5** (6 kcal/mol) with *eq* N7 and *ax* N6 atoms. Remarkably, compound **S9** ( $-7$  kcal/mol) with bridging Ade-N7,N6 is the most stable

species among all considered in this work. Its free energy of  $-7$  kcal/mol relative to the reactants corresponds to a free energy of  $-18$  kcal/mol relative to the free **S** tautomer.

**Comparison of Ade vs Gua Binding.** Comparing the results for both purine bases reveals marked differences in their thermodynamic binding preferences to the metal–metal unit of the dirhodium anticancer complex (Figures 3, 4, and 5): As is shown in Figure 3, *ax* Ade-N7 binding in **C2** ( $-4$  kcal/mol) is *more* favorable than *ax* Gua-N7 binding (0 kcal/mol). This result is corroborated by the experimental finding that *ax* Ade-N7 species were isolated and well-characterized, but *ax* Gua-N7 species of dirhodium tetracarboxylates were not.<sup>3,4,18</sup> In contrast, *eq* Ade-N7 binding, e.g., in **C4** (5 kcal/mol), is *less* favorable than *eq* Gua-N7 binding (2 kcal/mol). However, *eq* Ade-N6 binding is much *more* favorable than *eq* Gua-O6 binding (Figure 4). As is shown in Figure 5, the most stable Ade-N7,N6 chelate is species **S13** with the N7 atom in the *ax* position, whereas the most stable Gua chelate is the species with N7 in the *eq* position. Finally, the stabilization of the adenine **S** tautomer in **S9** when bridging the metal–metal bond via site N7 and N6 amounts to as much as  $-18$  kcal/mol and is more than three times stronger than the stabilization of Gua-N7,O6 when bridging the same metal–metal bond (Figure 5).

(29) As Pt–H–OH hydrogen bonds were predicted (Kozelka, J.; Berges, J.; Attias, R.; Fraitaig, J. *Angew. Chem., Int. Ed.* **2000**, *39*, 198), we have searched for metallo-hydrogen bonds of the type Rh–H–N but cannot provide any evidence for such interactions.

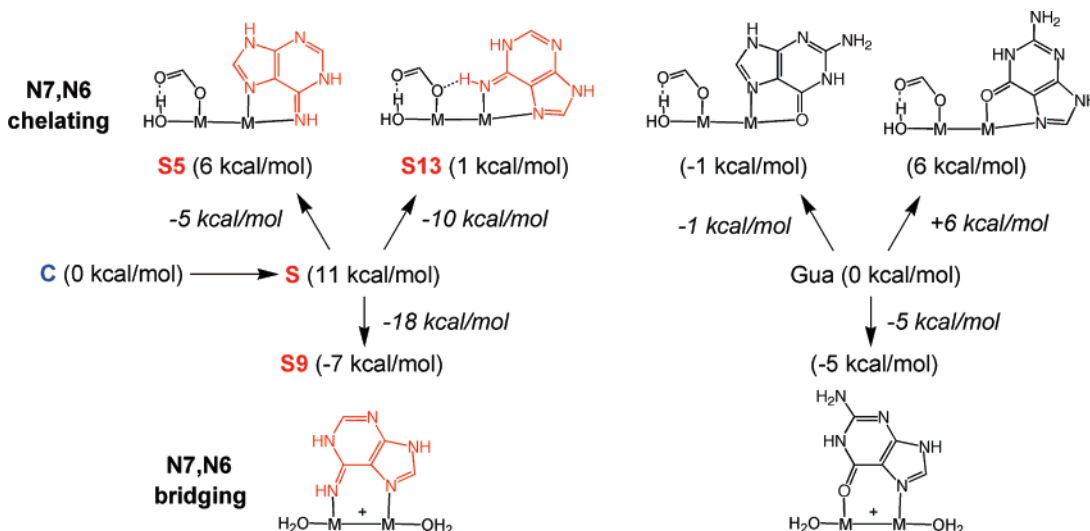


**Figure 5.** Axial–equatorial N7,N6 chelating and equatorial N7,N6 bridging of **S** (red). Gua–N7,O6 binding (black) is given for comparison. Molecular free energies in parentheses; differences in italics.

### 3. Key Transition States and Reaction Mechanisms

The Ade–N7,N6 species **S9** is clearly the most stable species in the reactions of Ade with **1**. Nevertheless, such a species with bridging Ade has not yet been reported experimentally for dirhodium tetracarboxylates, indicating that the formation of **S9** is kinetically very challenging. We have explored various pathways from the reactants (**1** + **C**) leading to **S9** including all relevant transition states for the kinetically controlled reaction steps.<sup>30</sup> The reactions are summarized in Figure S-1. Due to limited journal space, we report only the two most relevant mechanisms revealed by the calculations (Figures 6 and 7).

**Mechanism I.** Mechanism I (Figure 6) starts with axial N7 binding of the canonical tautomer **C** to **1**, yielding the *ax* Ade–N7 adduct **C2**. The reaction continues via *ax* to *eq* migration of the nucleobase via **TS C2 C3**, yielding the *eq* Ade–N7 adduct **C3**.<sup>31</sup> As **C3** contains a weak C–H–O hydrogen bond involving the nucleobase and the carboxylate, it may rearrange quickly to the more stable species **C4**, which contains an O–H–O hydrogen bond (Figure 6). An axial water may leave, leading to the *ax*–*eq* carboxylate chelate **C6**. The calculations reveal that a tautomerization can occur only in the *eq* Ade–N7 adducts: In **C4** or **C6**, a proton is transferred from N6 to N1, yielding **S4** or **S6**. The **S** tautomer may also form *ax*–*eq* nucleobase chelates **S5** and **S7**. The reaction continues via **S6**: The nucleobase rotates about the metal–N7 bond, and the N6 site binds via **TS S6 S8** to the second metal center, establishing the bridging Ade ligand in **S8**. The final step is the exchange of the *ax* carboxylate by an *ax* water to afford the product **S9**.

**Mechanism II.** Surprisingly, mechanism II (Figure 7) starts via *ax* binding of canonical (**C**) adenine via the amino group at

N6, yielding **C10**. The reaction may proceed via the species shown in Figure 7 in blue: **C10** can even undergo *ax* to *eq* migration of the nucleobase via **TS C10 C11**, yielding the *eq* adduct **C11**. **C11** may rearrange quickly to the more stable isomer **C12**. Then **C** → **S** tautomerization can occur, yielding **S12**. A variant of this mechanism involves the species shown in Figure 7 in green: In species **C10**, **C** → **A** tautomerization may occur to afford **A10**. **A10** undergoes *ax* to *eq* migration via **TS A10 A11** yielding **A11**. Then species **A12** is formed, which can tautomerize to **S12**. The reaction proceeds further via **S12** and the other species shown in red. In **S14**, rotation about the metal–N6 bond and binding of N7 to the second metal center via **TS S14 S16** yields **S16**. The *ax* carboxylate in **S16** is exchanged by an *ax* water to afford the product **S9**.

**Intermolecular vs Intramolecular Tautomerization.** We shall briefly comment on the mechanism of the nucleobase tautomerizations. Such dual proton transfers are commonly assumed to be fast, as they can occur via *intermolecular* protonation/deprotonation mechanisms.<sup>21</sup> We fully agree with this assumption in the case of **C** → **A** and **C** → **S** tautomerizations of adenine, where N1 becomes protonated and N6 becomes deprotonated. However, the **A** → **S** tautomerization of N6-metalated adenine is a rather different reaction: It proceeds via rotation about the C6=N6 bond, which likely has some double-bond character. A typical transition state for this *intramolecular* mechanism is **TS A12 S12** displayed in Figure 7; we predict an activation barrier of ~17 kcal/mol for this event.

**Free Energy Profile.** Figure 8 displays at a glance the free energies of all species assembled to a reaction profile for both mechanisms. Mechanism I starts in the middle and ends on the right; mechanism II starts in the middle and ends on the left. Both mechanisms include two reaction steps that are kinetically controlled. The first is *ax* to *eq* nucleobase migration, and the second is the cyclization to afford the bridging adenine species. For mechanism I, the TS migration **TS C2 C3** (21 kcal/mol) has a moderate free energy, but the TS cyclization **TS S6 S8** (32 kcal/mol) has a prohibitively high free energy. In contrast, in mechanism II, the relevant TS have a free energy of 26–27 kcal/mol: Both TS migration, **TS C10 C11** (26 kcal/mol) and

(30) The reactions involving only axial ligand exchange or intermolecular tautomerization events are expected to be fast, reversible, and thus thermodynamically controlled; cf. Pittet, P.-A.; Daddi, L.; Zbinden, P.; Abou-Hamdan, A.; Merbach, A. E. *Inorg. Chim. Acta* **1993**, *206*, 135.

(31) The reaction via **TS C2 C3** leads to **C3** via an additional intermediate that is similar to **C3** but contains only one axial aqua ligand and one free axial coordination site. Note that we determined the radius of the Rh atoms in the continuum dielectric model by matching the relative free energies in solution of several dirhodium complexes containing one axial aqua ligand and one free axial coordination site to the relative free energies in solution of the analogues complexes containing two axial aqua ligands (see Computational Details). Therefore, the current approach does not distinguish between **C3** and a similar structure that contains only one axial water.

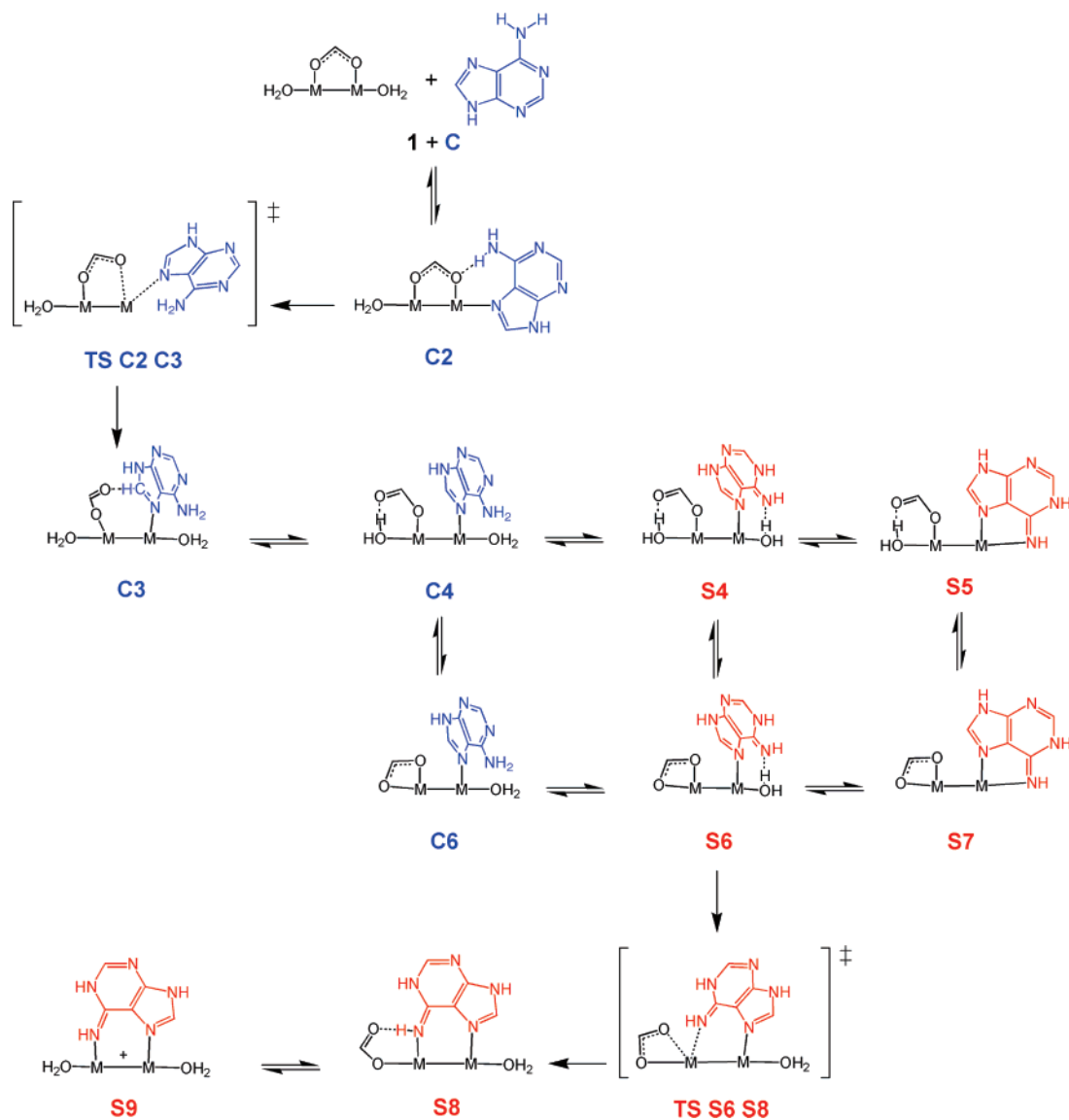


Figure 6. Mechanism I.

TS A10 A11 (26 kcal/mol), and TS cyclization, TS S14 S16 (27 kcal/mol). These free energy profiles favor mechanism II to mechanism I. A general problem for both pathways arises from the rapid formation of the *ax* Ade-N7 adduct **C2** (−4 kcal/mol). **C2** is more stable than the reactants, thus increasing the effective activation barriers by 4 kcal/mol and trapping the compounds in a thermodynamic sink. This result implies that the Ade reaction with **1** yielding **S9** would have to pass effective barriers of 30–31 kcal/mol in mechanism II. In contrast, the free energy of the TS for the Gua reaction with **1** was predicted to be ~25 kcal/mol, and there is no such thermodynamic sink. The 5–6 kcal/mol difference between the relevant transition states for the Ade and Gua reactions translates to a ratio of reaction rates of ~4 orders of magnitude. Thus, the Ade reaction with dirhodium tetraformate affords the *ax* Ade-N7 adduct **C2** (−4 kcal/mol) and will not proceed under reasonable conditions to the bridging Ade-N7,N6 species **S9** (−7 kcal/mol), although the latter is overall the most stable compound. It becomes clear that the metal–metal unit has to be modified to lower the activation barriers and to facilitate the reaction.

#### 4. Control of the Free Energy Profile via Modifying the Metal–Metal Unit

Our prediction that Ade binding to  $[\text{Rh}_2(\mu\text{-O}_2\text{CH})_4(\text{OH}_2)_2]$  (**1**) affording the bridging N7,N6 species **S9** is slower than the Gua reaction by some 4 orders of magnitude is interesting in light of the experimentally known reaction of dirhodium tetracarboxylates with Gua to afford the bridging Gua-N7,O6 species.<sup>14,19</sup> In this section, we report concepts toward rational control of reactivity by modifying the metal–metal unit with the ultimate goal to afford the bridging Ade-N7,N6 species. Considering our computational resources, we focus on the important question as to how much the highest transition state, i.e., the TS cyclization, can be lowered. Recent experimental work<sup>32</sup> succeeded in the synthesis of  $[\text{Rh}_2(\text{DTolF})_2(\text{d}(\text{ApA}))]$  (DTolF = *N,N'*-di-*para*-tolylformamidinate) from *cis*- $[\text{Rh}_2(\text{DTolF})_2(\text{NCCCH}_3)_6](\text{BF}_4)_2$  and d(ApA); NMR experiments<sup>32</sup> demonstrate N7,N6-bridging of the **S** rare tautomer in both adenine bases, which are in a head-to-head<sup>33</sup> conformation. As

(32) Chifotides, H. T.; Dunbar, K. R. *J. Am. Chem. Soc.* **2007**, *129*, 12480.

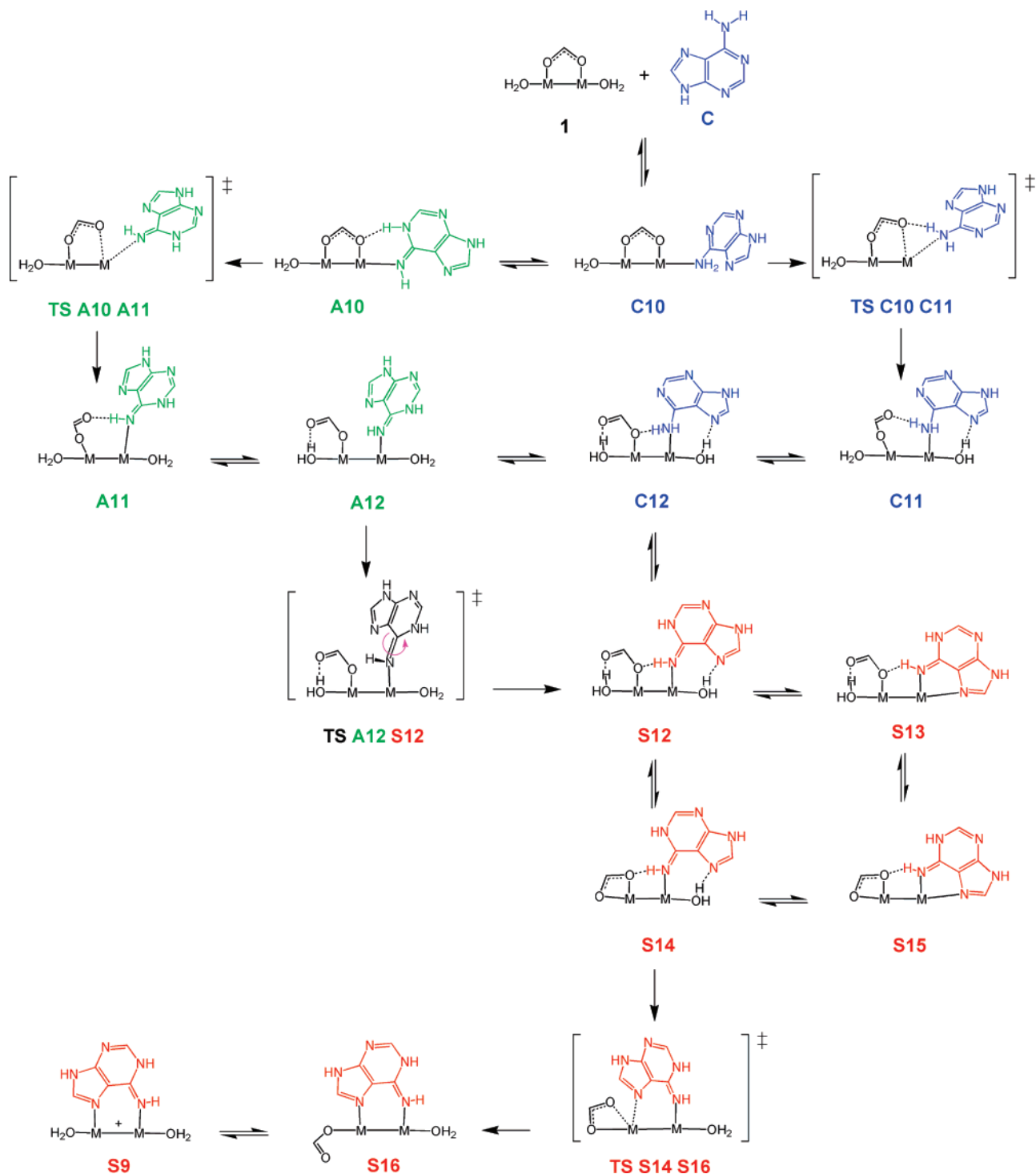


Figure 7. Mechanism II.

the reaction with adjacent AA sites is an unexplored venue in the chemistry of other DNA-binding anticancer agents such as cisplatin<sup>34</sup> and Ru-arene-en complexes,<sup>35</sup> systematic insights into rational control of reactivity are desirable and can contribute to the future design of dirhodium anticancer complexes.

- (33) (a) Kozelka, J.; Fouchet, M.-H.; Chottard, J.-C. *Eur. J. Biochem.* **1992**, *205*, 895. (b) Ano, S. O.; Intini, F. P.; Natile, G.; Marzilli, L. G. *J. Am. Chem. Soc.* **1998**, *120*, 12017.
- (34) (a) Bancroft, D. P.; Lepre, C. A.; Lippard, S. J. *J. Am. Chem. Soc.* **1990**, *112*, 6860. (b) Arpalathi, J.; Lippert, B. *Inorg. Chem.* **1990**, *29*, 104.
- (35) (a) Chen, H. M.; Parkinson, J. A.; Morris, R. E.; Sadler, P. J. *J. Am. Chem. Soc.* **2003**, *125*, 173. (b) Yan, Y. K.; Melchart, M.; Habtemariam, A.; Sadler, P. J. *Chem. Commun.* **2005**, 4764.

**Labile Leaving Groups.** To lower the free energies of transition states, one may consider more labile leaving groups. Because trifluoroacetic acid is  $-4$  pK<sub>a</sub> units more acidic than formic acid,<sup>3</sup> trifluoroacetate is less basic than formate and thus a better leaving group in dirhodium complexes. Figure 9a displays a simplified free energy profile for adenine binding to [Rh<sub>2</sub>(μ-O<sub>2</sub>CCF<sub>3</sub>)<sub>4</sub>(OH<sub>2</sub>)<sub>2</sub>]; note that only selected intermediates and TSs are shown, and the reaction of [Rh<sub>2</sub>(μ-O<sub>2</sub>CH)<sub>4</sub>(OH<sub>2</sub>)<sub>2</sub>] (**1**) is used as a reference. The calculations reveal that the free energy of the *ax* N7 adduct does not change (difference to reference: 0 kcal/mol), but the *eq* N7 and *eq* N7,N6-adducts



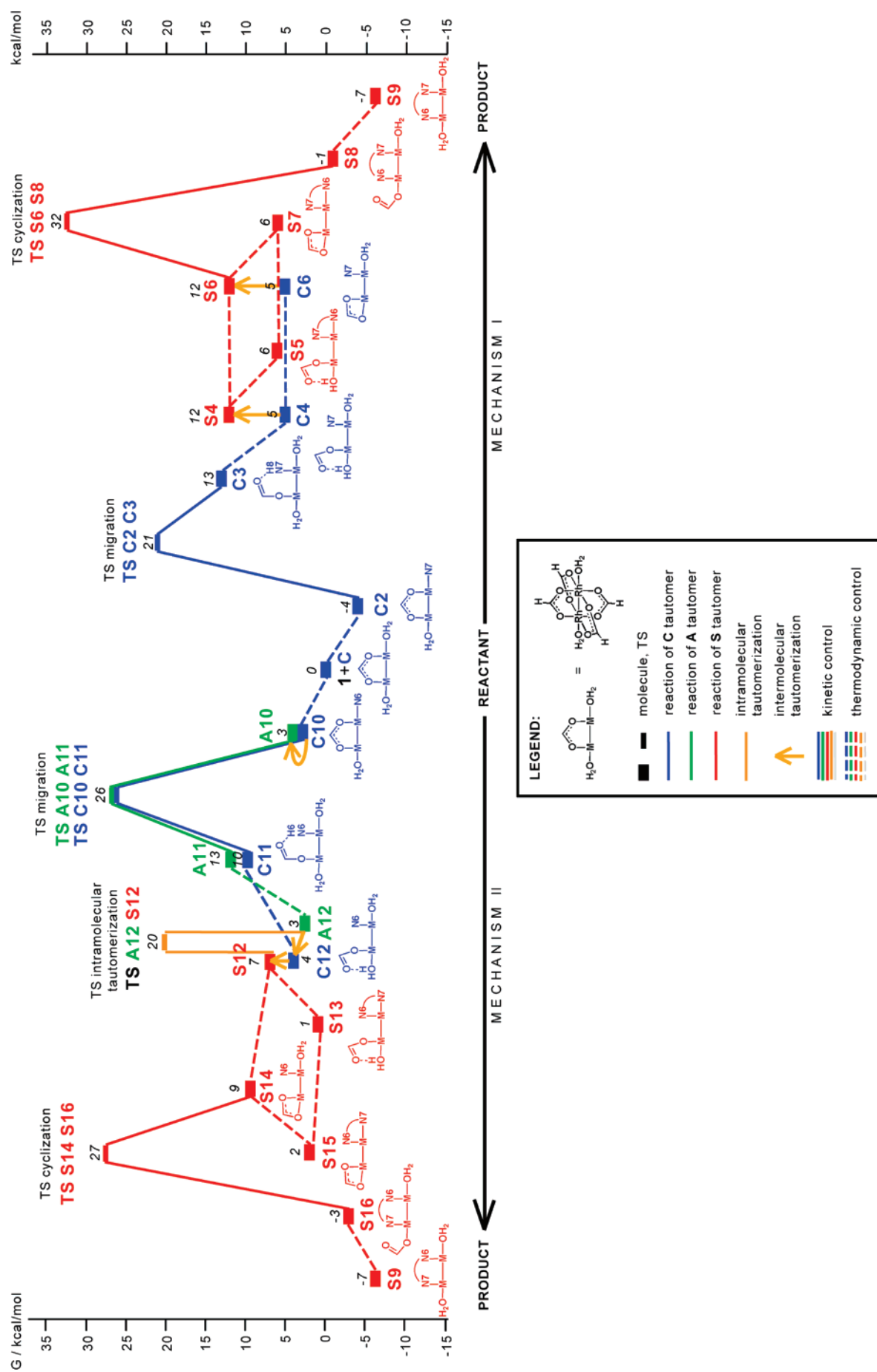


**Figure 8.** Free energy profile for mechanism I (from middle to right) and mechanism II (from middle to left). Thick and thin bars represent molecules and transition states, respectively. Dashed and solid lines represent thermodynamically and kinetically controlled reactions, respectively. A complete free energy profile is given in Figure S-1.

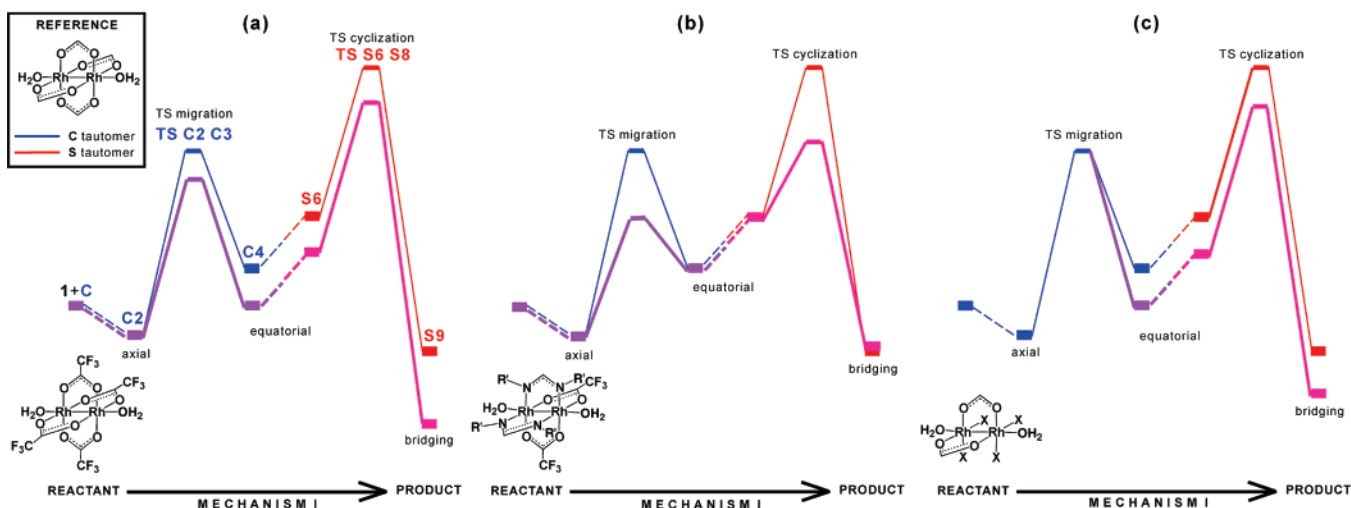


**Figure 9.** Simplified free energy profiles illustrating strategies to control the reaction leading to the stabilization of the **S** tautomer via binding to the metal–metal unit. (a) Labile leaving groups. (b) Two labile leaving groups and two trans-labilizing ligands. (c) Monodentate leaving groups. The predicted free energy profile for Ade binding to dirhodium tetraformate is shown as a reference in blue and red; the predicted free energy changes upon modification of the metal–metal unit are shown in violet and pink. The figure refers to mechanism I, but similar strategies may apply to mechanism II.

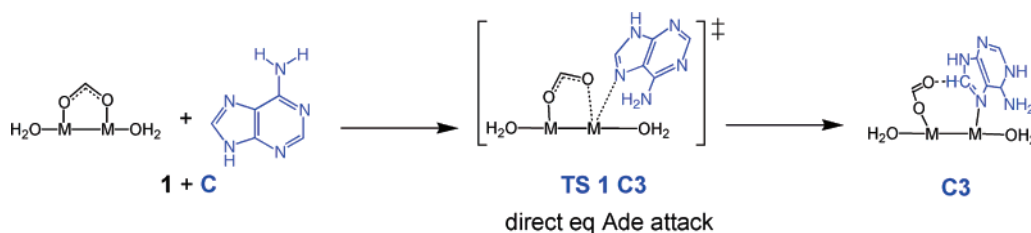


**Figure 10.** Direct equatorial adenine attack.

become much more stable (diff.  $-5$  and  $-10$  kcal/mol, respectively). The transition states clearly benefit from the trifluoroacetate leaving group as well, as is demonstrated by the calculated stabilization of the highest TS, i.e., the TS for cyclization (difference to reference:  $-5$  kcal/mol).

**Trans-Labilizing Ligands.** To enhance the lability of the leaving groups further, one may place strong ligands trans to the leaving groups. Importantly, it was experimentally observed<sup>3,4</sup> that up to two carboxylates at the metal–metal unit can be displaced by nucleobases, suggesting the enhanced lability of the *two* leaving carboxylates by *two* strong trans ligands. The ligands capable of bridging the metal–metal unit are not limited to OO-type ligands such as carboxylates, but a large array of NN-type, SS-type, and mixed ligands is available.<sup>4</sup> Due to the current interest in NN-type ligands including formamidinate groups,<sup>3–5,20,32</sup> we have considered the reaction of  $[\text{Rh}_2(\mu\text{-O}_2\text{CCF}_3)_2(\mu\text{-NMe})_2\text{CH})_2(\text{OH}_2)_2]$ , which contains two *N,N'*-dimethyl formamidinate ligands (Figure 9b). The changes in the reaction profile relative to the reference reaction of  $[\text{Rh}_2(\mu\text{-O}_2\text{CH})_4(\text{OH}_2)_2]$  are remarkable: The overall thermodynamics of the reaction yielding the bridging Ade-N7,N6 product remains nearly unaffected (difference to reference: 0 kcal/mol). However, the transition states gain significantly from the NN-type ligands *trans* to the leaving groups, as is demonstrated by the calculated stabilization of the highest TS, i.e., the TS for cyclization (difference to reference:  $-10$  kcal/mol).

**Monodentate Leaving Groups.** To lower the transition state of the second step (TS for cyclization), monodentate leaving groups may be used. One monodentate ligand will be released into solution already after the first step, *ax* to *eq* migration. The

consequences of the reaction are shown in Figure 9c.<sup>36</sup> In the case of the *ax* intermediates and the TS migration, there is no additional molecule/ion in solution, so one expects only minor entropic changes. In case of *eq* intermediates and the TS cyclization, however, a monodentate leaving group has been fully released, and there is one additional molecule/ion in solution. This complete release of the leaving group will increase the translational and (if applicable) rotational entropy and will decrease at physiological temperature the free energy of the *eq* intermediates and of the TS for cyclization. For example, the predicted free energy contribution from the translational entropy of a free chloride ion amounts to  $-11$  kcal/mol in vacuo and possibly half<sup>45</sup> of this amount in aqueous solution.

**Blocking Axial Sites.** As the *ax* Ade-N7 adduct **C2** constitutes a thermodynamic sink in the reaction affording the N7,-N6-bridging **S** tautomer, one may believe that eliminating this sink by blocking the axial coordination sites of the dirhodium

- (36) The estimated profile in Figure 9c considers only entropic changes of the reaction and refers to hypothetical leaving groups that have the same metal–bond strengths as the metal–carboxylate bonds and the same hydrogen-bonding preferences with the Ade tautomers. If leaving groups are chosen that lack good hydrogen-bond acceptors, the axial Ade-N7 adduct may be destabilized, eliminating a thermodynamic sink from the reaction.
- (37) For example, the standard reaction free energy of ATP hydrolysis yielding ADP is  $-7.3$  kcal/mol. Berg, J. M.; Tymoczko, J. L.; Stryer, L. *Biochemistry*, 5th ed.; W. H. Freeman: New York, 2002; p 376.
- (38) Frisch, M. J. et al. *Gaussian 03*, revision D.01; Gaussian, Inc.: Wallingford, CT, 2004 (www.gaussian.com).
- (39) Hay, P. J.; Wadt, W. R. *J. Chem. Phys.* **1985**, *82*, 299.
- (40) (a) Binkley, J. S.; Pople, J. A.; Hehre, W. J. *J. Am. Chem. Soc.* **1980**, *102*, 939. (b) Hehre, W. J.; Ditchfield, R.; Pople, J. A. *J. Chem. Phys.* **1972**, *56*, 2257.
- (41) Ehlers, A. W.; Böhme, M.; Dapprich, S.; Gobbi, A.; Höllwarth, A.; Jonas, V.; Köhler, K. F.; Stegmann, R.; Veldkamp, A.; Frenking, G. *Chem. Phys. Lett.* **1993**, *208*, 111.

unit may facilitate the reaction. However, blocking the *ax* binding sites would lead to a change in the mechanism, because the pathway for *ax* to *eq* migration is also eliminated. We have investigated the direct equatorial Ade attack on **1** as an alternative mechanism (Figure 10) and find that the corresponding transition state **TS 1 C3** (30 kcal/mol) has a 9 kcal/mol higher free energy than the TS for *ax* to *eq* migration **TS C2 C3** (21 kcal/mol). We do not consider blocking *ax* sites a viable strategy to promote the formation of the N7,N6-bridging **S** tautomer.

## 5. Biological Implications and Concluding Remarks

In this work, we have investigated the binding of three adenine (Ade) tautomers to metal–metal bonded dirhodium(II) antitumor agents using high-level quantum chemical calculations.<sup>3–10</sup> As compared to the simple ligand substitutions of cisplatin,<sup>11,12</sup> calculations play a unique role in the investigation and future design of dirhodium antitumor complexes, because most key intermediates in the reactions are predicted to be slightly less stable than the reactants and thus extremely difficult to characterize or isolate experimentally. The results of this work and their biological relevance can be summarized as follows.

1. To obtain the N6-imino rare forms of adenine (**A** and **S**) from the free canonical form (**C**), a tautomerization free energy of 9 and 11 kcal/mol, respectively, must be invested in aqueous solution. These values are rather high as compared to typical biological free energy scales,<sup>37</sup> demonstrating the challenge of stabilizing the rare tautomers upon metalation. Investigation of various Ade adducts with dirhodium tetraformate reveals that the overall most stable species is an adduct in which the **S** tautomer bridges the metal–metal bond via sites N7 and N6. The stabilization of the **S** tautomer in this N7,N6-bridging adduct amounts to as much as –18 kcal/mol, thus exceeding the stabilization of N7,O6-bridging guanine by a factor of 3. All other binding modes of adenine, including the well-known axial N7 binding of the **C** form, are predicted not to be thermodynamically competitive to the N7,N6-bridging **S** tautomer.

2. Rigorous transition state predictions for multiple reaction pathways between dirhodium tetraformate and the three Ade tautomers suggested two mechanisms leading to the N7,N6-bridging **S** tautomer. Mechanism I starts with *ax* binding of **C** via site N7, nucleobase migration to the *eq* position, and subsequent **C** → **S** tautomerization. Remarkably, mechanism II starts with *ax* binding of **C** via the N6-amino group. Tautomerization in the *ax* N6 adduct to afford the **A** form is optional in this mechanism, but tautomerization in the *eq* N6 adduct to afford the **S** form after nucleobase migration is mandatory. The final step in both mechanisms is the cyclization of the monodentate N7 or N6 adduct to afford the N7,N6-bridging **S**

tautomer. Mechanism I has a higher overall barrier than mechanism II, but all metal binding sites involved in mechanism I are located in the major groove of double-stranded DNA. In contrast, mechanism II proceeds via initial N6 binding of the **C** or **A** tautomer and would interfere with base pairing or stacking. Therefore, mechanism II remains plausible for single-stranded DNA or RNA rather than for undistorted double-stranded DNA. Both mechanisms for adenine binding to dirhodium tetraformate have significantly higher effective barriers than does the guanine reaction, calling for strategies to lower the barriers via modifying the metal–metal unit.

3. The metal–metal unit allows chemists to use an immense toolbox of ligands to tune the reactivity of the dirhodium antitumor complexes toward the formation of the N7,N6-bridging **S** tautomer. Concepts to modify the metal–metal unit with the ultimate goal to lower the free energy of the highest transition states include (a) the use of more labile leaving groups, (b) particularly in combination with trans-labilizing ligands, and (c) the use of monodentate leaving groups. Such approaches lower the effective barrier by approximately 4–10 kcal/mol, while the product with the N7,N6-bridging **S** tautomer is as stable as or more stable than the analogue compound in the reaction of dirhodium tetraformate. In contrast, blocking the axial coordination site to eliminate the thermodynamic sink of axial Ade-N7 adducts of the **C** tautomer is not a viable option to promote the reaction, as the lack of axial binding sites would cause the reaction to switch to a different mechanism with high-lying transition states.

## 6. Computational Details

The geometries of the molecules and transition states (TS) were optimized at the gradient-corrected DFT level using the three-parameter fit of exchange and correlation functionals of Becke (B3LYP),<sup>26</sup> which includes the correlation functional of Lee, Yang, and Parr (LYP),<sup>27</sup> as implemented in Gaussian 03.<sup>38</sup> The LANL2DZ ECPs<sup>39</sup> and valence-basis sets were used for the metal, and the 6-31G(d,p) basis sets were used for the other atoms.<sup>40</sup> This basis-set combination is denoted II. Vibrational frequencies were also calculated at B3LYP/II; all structures reported herein are either minima or first-order saddle points on the potential energy surfaces. Improved total energies were calculated at the B3LYP level using the same ECP and valence-basis set at the metal, but totally uncontracted and augmented with a set of f functions,<sup>41</sup> together with the 6-311+G(d,p) basis sets at the other atoms. This basis-set combination is denoted III+. Free energies were calculated by adding corrections from unscaled zero-point energy (ZPE), thermal energy, work, and entropy evaluated at the B3LYP/II level at 298.15 K, 1 atm to the energies calculated at the B3LYP/III+//II level.<sup>42</sup>

Solvation free energies of the structures optimized at the B3LYP/II level were calculated by a Poisson–Boltzmann finite element method (PBF) with a dielectric constant  $\epsilon$  of the dielectric continuum that represents the solvent. The PBF calculations were performed at the B3LYP level using the LACVP\*\* basis set at the metal and the 6-31G(d,p) basis set at the other atoms, as implemented in the Jaguar program package.<sup>43</sup> The continuum boundary in the PBF calculations was defined by a solvent-accessible molecular surface with a set of atomic radii<sup>44</sup> for H (1.150 Å), C (1.900 Å), N (1.600 Å), O (1.600 Å), and Rh (1.600 Å). The radius at Rh was determined by matching the calculated relative free energy in solution of several dirhodium complexes with one *ax* aqua ligand and one free *ax* coordination site to the calculated relative free energy in solution of the analogous complexes with two *ax* aqua ligands. The radii at the other atoms were employed for our previous works. We believe that continuum dielectric models do not properly

(42) As the energy gap in **1** between the HOMO (a  $\pi^*$  orbital of the Rh–Rh bond) and the LUMO ( $\sigma^*$  orbital of the Rh–Rh bond) is as large as 4.0 eV, we did not consider the involvement of excited states in the reactions with nucleobases. Note that dirhodium complexes are also developed as photoactivated cisplatin analogues (Lutterman, D. A.; Fu, P. K. L.; Turro, C. J. *Am. Chem. Soc.* **2006**, *128*, 738).  $\text{Rh}_2(\pi^*) \rightarrow \text{Rh}_2(\sigma^*)$  transitions were predicted to occur at a wavelength of less than 600 nm, which corresponds to an energy higher than 47 kcal/mol.

(43) *Jaguar*, version 7.0; Schrödinger, LCC: New York, 2007 ([www.schrodinger.com](http://www.schrodinger.com)).

(44) (a) Rashin, A. A.; Honig, B. *J. Phys. Chem.* **1985**, *89*, 5588. (b) Baik, M. H.; Friesner, R. A. *J. Phys. Chem. A* **2002**, *106*, 7407.

(45) (a) Wertz, D. H. *J. Am. Chem. Soc.* **1980**, *102*, 5316. (b) Abraham, M. H. *J. Am. Chem. Soc.* **1981**, *103*, 6742.

describe the changes in solvation entropy in bimolecular reactions, as comparisons with experimental values indicated that relative free energies of reactions of Pt(II), Pd(II), and Ru(II) complexes with biomolecules are systematically  $\sim 6$  kcal/mol too high. According to Wertz and others,<sup>45</sup> various molecules lose a constant fraction (approximately 0.5) of their entropy, when they are dissolved in water. All free energies in solution were modified by an entropic term that is half (0.5) of the entropy in vacuo with the opposite sign. This empirical correction has led to predicted reaction and activation free energies for the reactions of metal complexes that are in good agreement with experimental values.<sup>46</sup>

(46) (a) Deubel, D. V.; Lau, J. K.-C. *Chem. Commun.* **2006**, 2451. (b) Lau, J. K.-C.; Deubel, D. V. *J. Chem. Theory Comput.* **2006**, 2, 103.

**Acknowledgment.** Financial support from the Fonds der Chemischen Industrie, Germany, the Austrian Science Foundation, and the Swiss Science Foundation is gratefully acknowledged. Computing time was provided by CSCS, Manno, Switzerland.

**Supporting Information Available:** Complete ref 38. Complete free energy profiles. Absolute energies (in Hartrees) and optimized geometries (as molecular graphics and Cartesian coordinates) of molecules and transition states. This material is available free of charge via <http://pubs.acs.org>.

JA076603T